

THE PHYSICAL REVIEW

A journal of experimental and theoretical physics established by E. L. Nichols in 1893

SECOND SERIES, Vol. 135, No. 3A

3 AUGUST 1964

Frequency Pushing and Frequency Pulling in a He-Ne Gas Optical Maser

R. A. MCFARLANE

Bell Telephone Laboratories, Murray Hill, New Jersey

(Received 16 March 1964)

Measurements have been made of the variation of beat frequency between two simultaneously oscillating axial modes of a He-Ne gas optical maser as their disposition with respect to line center was continuously varied and as the discharge excitation level was increased above beat threshold for fixed mode positions. The results are compared with the theory of Lamb. The present calculations ignore mode interaction effects which are, however, included in Lamb's theory. The effects of frequency pushing, frequency pulling, and "hole repulsion" are apparent in the measurements as well as an excitation-dependent linewidth.

MEASUREMENTS have been made of the beat frequency between adjacent axial modes of a He-Ne gas optical maser as the cavity resonances were scanned across the Doppler broadened gain curve and as the excitation level was varied. The results are compared with the theory of W. E. Lamb, Jr.¹ The present calculations ignore mode-interaction effects which are included in Lamb's theory as mode-amplitude information that was not available in the experiment. Nevertheless, there is qualitative agreement when the appropriate assumption is made for the value of the natural linewidth. Nonlinear effects² at higher levels of excitation are apparent in the measurements.

The maser employed in the experiment operated at $1.15\ \mu$ and used a plane-parallel mirror configuration with the mirrors inside the vacuum envelope and spaced approximately $\frac{1}{2}$ m. The cavity length was varied magnetostrictively³ and could be scanned over three adjacent axial modes. With naturally occurring neon, the mixture of isotopes results in a line asymmetry^{4,5} which makes interpretation of the results difficult. For this reason all of the work with the exception of one preliminary experiment on scanning the cavity length

was done with enriched Ne²² isotope. Gas pressures were He 1.1 mm and Ne²² 0.11 mm.

The measurement system is shown in Fig. 1. The maser output fell on the photocathode of a 7102 photomultiplier tube from which a 306-Mc/sec beat signal was sent to the frequency measuring and recording equipment. As the outputs of the two axial modes were orthogonally polarized, a linear polaroid was placed between the maser and the photomultiplier in order to observe a beat.² The frequency was measured with a Hewlett-Packard Model 540 B transfer oscillator and

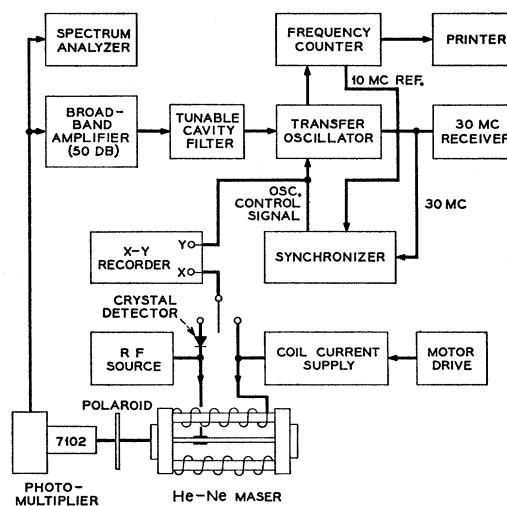


FIG. 1. Block diagram of measuring equipment.

¹ W. E. Lamb, Jr., *Phys. Rev.* **134**, A1429 (1964). The main results of the paper were reported at the Third International Conference on Quantum Electronics, Paris, February, 1963 (unpublished).

² W. R. Bennett, Jr., *Phys. Rev.* **126**, 580 (1962).

³ W. R. Bennett, Jr., and P. J. Kindlmann, *Rev. Sci. Instr.* **33**, 601 (1962).

⁴ R. A. McFarlane, W. R. Bennett, Jr. and W. E. Lamb, Jr., *Appl. Phys. Letters* **2**, 189 (1963).

⁵ A. Szöke and A. Javan, *Phys. Rev. Letters* **10**, 521 (1963).

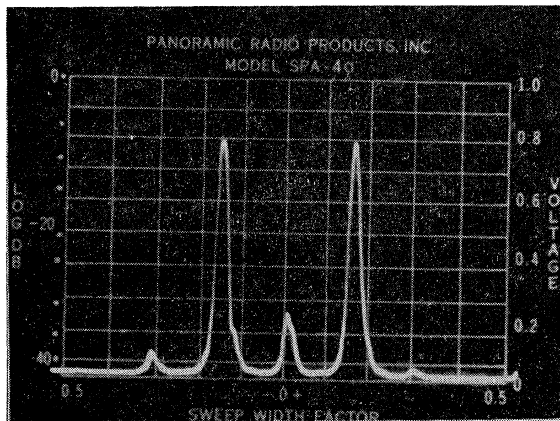


FIG. 2. Panoramic receiver display of five beat components at 306 Mc/sec. Total scan is approximately 20 kc/sec.

Model 524 D frequency counter using a Dymec Model 5796 synchronizer. The deviation output voltage of the synchronizer was recorded to give a continuous plot of the beat frequency as the maser length or excitation was varied and the printer provided calibration information.

The experiments were done with sufficient excitation to obtain oscillation on two adjacent axial modes. The value of $c/2L$, the mode separation, as determined from the measured mirror spacing was 306.440 ± 0.048 Mc/sec. Frequency-pulling effects reduce this difference to the vicinity of 306.0 Mc/sec, the shift in beat frequency depending upon the excitation level and the disposition of the two cavity resonances with respect to the line center.

First observations of the 306 Mc/sec beat on a spectrum analyzer showed it to have five components. In Fig. 2 these components are shown with a total fre-

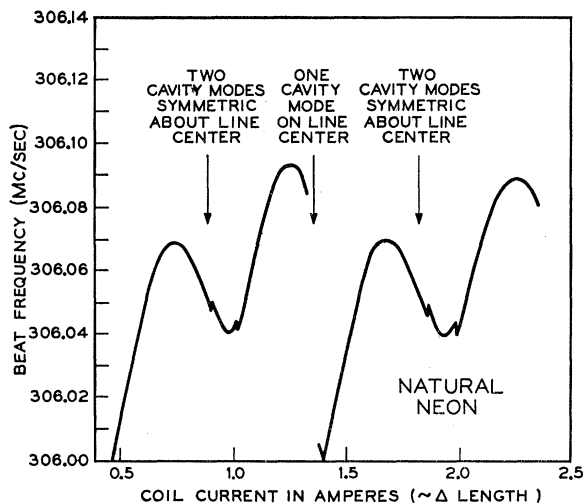


FIG. 3. Variation of beat frequency between two adjacent axial modes as the cavity length was increased by approximately λ . The maser contained natural neon.

quency scan width of approximately 20 kc/sec. The individual components are spaced about 3.3 kc/sec and in some cases suggest an unresolved structure. Rotation of a quarter-wave plate placed between the maser and the linear polaroid caused elimination of some components and enhancement of others. A note on the details of this experiment is being prepared. The five-component structure is interpreted as indicating simultaneous oscillation with left-circular, linear, and right-circular polarization at each of the two cavity resonances. A small stray nonaxial magnetic field caused a Zeeman splitting of the emission components^{6,7} the splitting being the same or nearly so at each cavity resonance. The five-component beat structure represents all possible beats in the vicinity of $c/2L$ between the six emission components. The addition of a mumetal shield around the discharge tube to eliminate this field, which

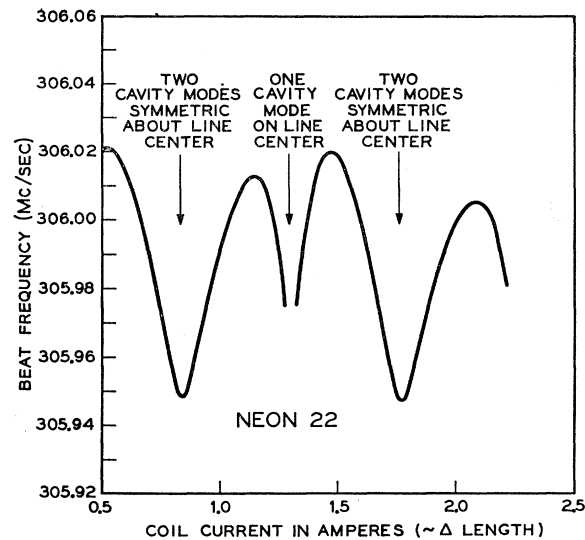


FIG. 4. Variation of beat frequency between two adjacent axial modes as the cavity length was increased by approximately λ . The maser contained enriched Ne^{22} .

had an order of magnitude of 1 G, resulted in a single-component beat. The radiation was then linearly polarized at each cavity resonance the directions of the modes being orthogonal.²

The length of the maser containing natural neon was scanned over several modes with the excitation level adjusted so that one mode just fell below threshold as the second mode crossed line center. The resulting variation of the beat frequency is shown in Fig. 3. No beat was present when one mode was at line center. As will be seen this curve should be symmetric about each of two limiting cases: one cavity mode at line center, and two cavity modes equally spaced from line

⁶ A. Javan (private communication).

⁷ H. Stutz, R. Paananen, and G. F. Koster, *J. Appl. Phys.* **33**, 2319 (1962).

center. The lack of such behavior in Fig. 3 is attributed to a line asymmetry due to the presence of several neon isotopes. Line-center power-dip measurements have also demonstrated this line asymmetry.^{4,5} At one portion of the scan there occurred discontinuous jumps in frequency of approximately 2 kc/sec. These exhibited a hysteresis effect with cavity length changes, their position depending upon the direction of the change. The record in Fig. 3 was made with increasing coil current. The discontinuities occur at currents approximately 0.1 A less as the scan is made with decreasing current. Similar discontinuities when three axial modes were oscillating showed abrupt changes in the polarization of one component.

The measurements were repeated using enriched Ne²² under similar conditions of excitation (17 W rf) and the beat-frequency variation with cavity length is shown in Fig. 4. The small asymmetry still present may be due to residual Ne²⁰. Repeating the measurement at lower levels of excitation resulted in similar curves somewhat shifted in frequency but with a beat note present over shorter regions of the length scan.

To observe power-dependent frequency effects the cavity length was fixed at several values between the two limiting cases for cavity-mode positions and the excitation increased. Several of the resulting curves are shown in Fig. 5 where the output from a crystal detec-

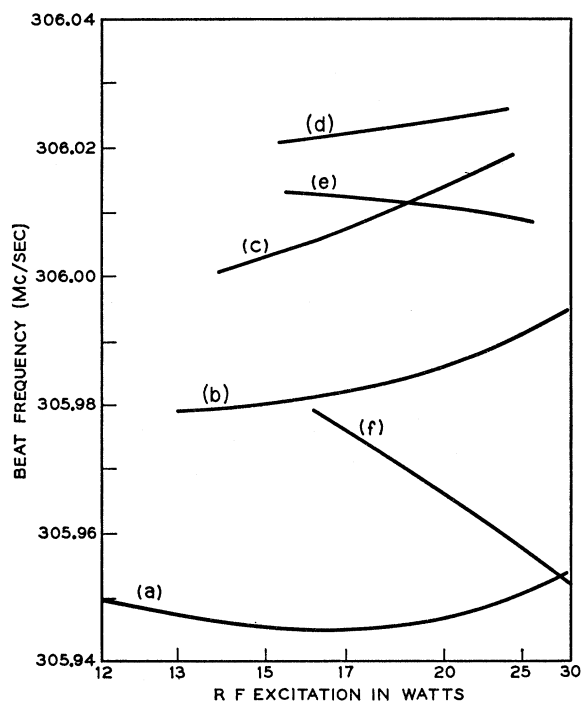


FIG. 5. Variation of beat frequency with excitation for different dispositions of two modes about line center. (a) -155.6 Mc/sec, +150.8 Mc/sec, (b) -119.7 Mc/sec, +186.7 Mc/sec, (c) -95.7 Mc/sec, +210.7 Mc/sec, (d) -47.9 Mc/sec, +258.5 Mc/sec, (e) -35.9 Mc/sec, +270.5 Mc/sec, (f) -12.0 Mc/sec, +294.4 Mc/sec.

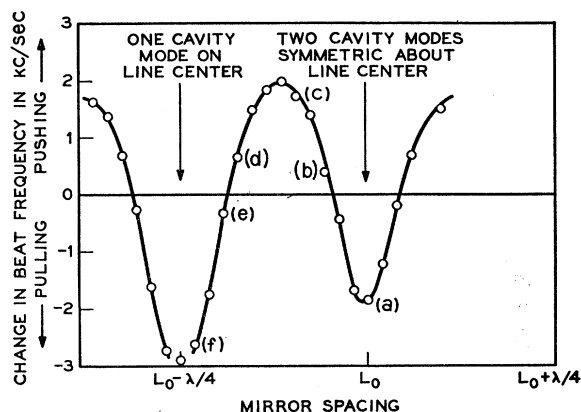


FIG. 6. Variation of initial slope of power dependent beat frequency curves. Of the several measurements made the letters identify those traced out in Fig. 5. Excitation increment is from threshold to 5% above threshold.

tor monitoring the rf level has been used to provide information on the level of excitation. Position (a) represents modes at -155.6 Mc/sec and +150.8 Mc/sec and is very close to the symmetric placement of two modes about line center. In this condition the beat frequency at threshold had a value smaller than that for any other placement of modes. As the excitation was raised, the beat frequency decreased indicating that the two frequencies of oscillation were moving toward line center. At higher levels of excitation the beat frequency increased with the oscillation frequencies moving away from line center toward their respective cavity resonances.

As the maser length was changed to place one cavity mode closer to line center, the curves (b)-(f) were obtained. It appears that there was one mirror spacing between (d) and (e) where the beat frequency would have been independent of the level of excitation. There was a continuous variation of initial slope as the modes were scanned from the symmetric condition to the position where one mode was very close to line center as represented by (f): modes at -12.0 Mc/sec and +294.4 Mc/sec. This is shown in Fig. 6 where the slope has been specified by the change in beat frequency corresponding to an increase in excitation from threshold level for the appearance of a beat to 5% above this threshold level. The initial slopes for those curves in Fig. 5 are identified in Fig. 6.

Lamb¹ has shown that under single-mode operation the frequency of oscillation ν can be written

$$\nu = \Omega + \sigma + \rho E^2, \quad (1)$$

where Ω is the resonant frequency of the optical cavity, σ is an excitation dependent term pulling the frequency of oscillation away from the cavity resonance toward line center, and ρE^2 is a term which depends upon the power in the mode and is of such a sign as to move the frequency of oscillation away from line center,

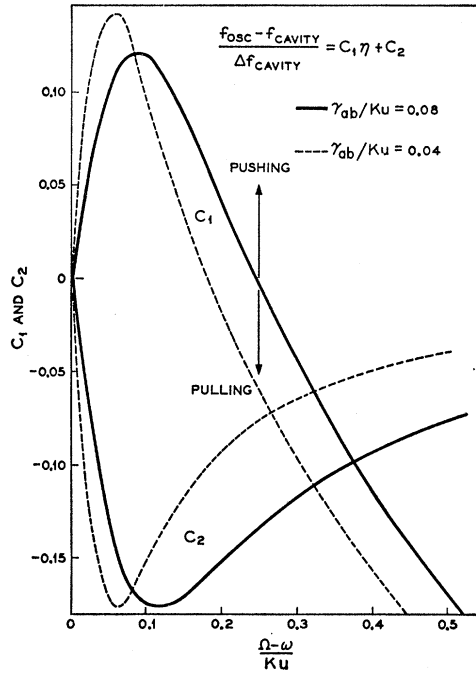


FIG. 7. The constants C_1 and C_2 of Eq. (2) as a function of $(\Omega - \omega)/Ku$: the frequency difference between the cavity resonance and line center/0.6 Doppler linewidth. For $C_1 > 0$ frequency pushing away from line center toward the cavity-resonant frequency occurs as excitation is increased. For $C_1 < 0$ frequency pulling toward line center occurs with increasing excitation. For the values of η used here the pulling term dominates and the oscillation frequency is always displaced from the cavity-resonant frequency toward line center.

The quantities σ and ρE^2 can be expressed as a function of η the relative excitation above threshold when tuned to line center and the frequency difference between the cavity resonance and line center. In the theory are two parameters: Ku , which is 0.6 times the Doppler width in rad/sec, and γ_{ab} , which is π times the natural linewidth of the transition. For the 1.15μ transition of neon and a Doppler linewidth of 1000 Mc/sec, Ku corresponds to a value of 600 Mc/sec. The value of γ_{ab} corresponds to a natural linewidth of several tens of megacycles. Values of 48 Mc/sec and 96 Mc/sec have been assumed in the present calculation. Szöke and Javan⁵ have shown that pressure effects require the introduction of an additional linewidth parameter, but this elaboration has not been introduced here into Lamb's formulation and the results must be considered in this light.

With the linear theory of Eq. (1) and the parameters assumed above, it is possible to write an expression for the oscillation frequency in terms of the relative excitation.

$$\frac{f_{\text{osc}} - f_{\text{cavity}}}{\Delta f_{\text{cavity}}} = C_1 \eta + C_2. \quad (2)$$

Δf_{cavity} is the optical cavity bandwidth and η is the

relative excitation

$$\eta = \bar{N} / \bar{N}_T, \quad (3)$$

where \bar{N} is the average of the population inversion density over the cavity and \bar{N}_T is the value of \bar{N} for threshold oscillation when the cavity frequency Ω is tuned to the peak frequency ω of the atomic resonance curve.

The constants C_1 and C_2 are plotted in Fig. 7 for $\Omega > \omega$. (For $\Omega < \omega$ the absolute direction of pushing or pulling reverses and C_1 and C_2 in Fig. 7 must be multiplied by -1 .) For a cavity resonance near line center the value of C_1 is positive indicating that frequency pushing is dominant with increasing excitation, while for a cavity resonance well removed from line center frequency pulling toward line center predominates with increasing excitation. The value of $(\Omega - \omega)/Ku$, where $C_1 = 0$, depends upon the assumed γ_{ab} , and this suggests that a value of γ_{ab} could be inferred from a measurement of cavity resonance offset from line center when the frequency of oscillation is observed to be independent of excitation.¹

In the Appendix, an analysis similar to that of Bennett² shows that σ can be identified as being due to a phase shift associated with the Gaussian gain profile and ρE^2 is a hole repulsion term where the presence of a complimentary hole in the gain profile results in a phase increment at the frequency of oscillation such as to move this frequency away from line center.

When two modes are oscillating, an additional mode interaction term is included in the frequency-determining equation.¹

$$\begin{aligned} \nu_1 &= \Omega_1 + \sigma_1 + \rho_1 E_1^2 + \tau_{12} E_2^2, \\ \nu_2 &= \Omega_2 + \sigma_2 + \rho_2 E_2^2 + \tau_{21} E_1^2. \end{aligned} \quad (4)$$

For the present work, however, no information was available on the amplitudes E_1 and E_2 and most of our calculations of $\nu_2 - \nu_1$ consider only the first-order result (1). In addition, the experiment involved orthogonally

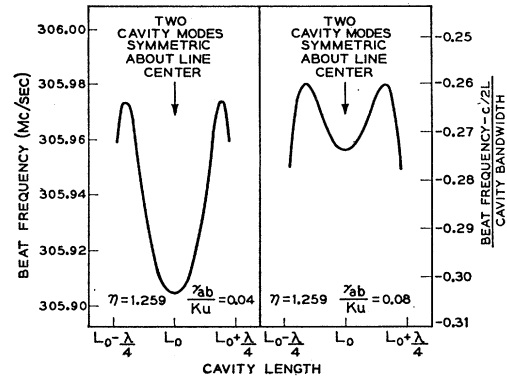
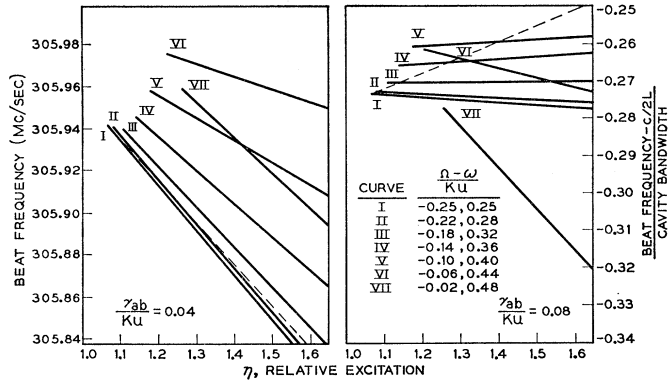


FIG. 8. Calculated variation with cavity length of beat frequency between two axial modes for two values of γ_{ab}/Ku assuming no mode interaction effects. The excitation is adjusted for oscillation threshold at $(\Omega - \omega)/Ku = \pm 0.48$. The frequency scale assumes a cavity bandwidth of 1.77 Mc/sec.

FIG. 9. Calculated variation with excitation η of beat frequency between two axial modes for the indicated mode positions and two values of γ_{ab}/Ku . The solid lines assume no mode interaction effects. The dashed curves include interaction effects for the symmetric case (I). The frequency scale assumes a cavity bandwidth of 1.77 Mc/sec.



polarized modes while the analysis has considered only parallel polarizations. The effect of this on τ_{12} and τ_{21} will be such as to reduce the mutual frequency pushing effects.⁸ Equation (4) can also be interpreted in terms of phase shifts but the presence of four holes in the gain curve is a substantial complication.

In Fig 8 is plotted the variation of beat frequency with cavity length calculated for two values of the ratio γ_{ab}/Ku . The approximation has been made that the mode spacing (306.440 Mc/sec) is equal to one-half Ku (600 Mc/sec). The frequency scan is from mode positions $-0.02 Ku$, $+0.48 Ku$ to $-0.48 Ku$, $+0.02 Ku$. The excitation η is adjusted for threshold at $\pm 0.48 Ku$ from the relation¹

$$\eta = \exp(\Omega - \omega)^2 / (Ku)^2, \quad (5)$$

where it has been assumed $\gamma_{ab} \approx 0$. Since the total beat frequency shift away from 306.440 Mc/sec is substantially larger than any variations with length and the threshold beat frequency for symmetric placement of modes is relatively independent of γ_{ab}/Ku , a reasonably accurate value of cavity bandwidth can be determined. From the measurements of this threshold beat frequency the cavity bandwidth was found to be 1.77 Mc/sec and the indicated frequency scale in Fig. 8 and 9 is based on this value. It is apparent from Fig. 7 that the rapid decrease of beat frequency as one mode approaches line center is due to the rapid decrease of frequency pushing associated with that mode.

Figure 9 shows the computed dependence of beat frequency on excitation for two values of the ratio γ_{ab}/Ku with the beat frequency excitation threshold determined from Eq. (5). The measured frequencies of the beat at threshold are observed to show a larger variation than is predicted by either set of curves. This is attributed to mode interaction or hole repulsion effects.

With the symmetric placement of two cavity resonances both modes cross threshold at the same time and E_1 and E_2 in Eq. (4) are small. The power present in one mode has little influence on the oscillation fre-

quency of the other mode. Lamb¹ finds in this special case that the frequency difference

$$\nu_2 - \nu_1 = \Omega_2 - \Omega_1 + \sigma_2 - \sigma_1 + 4\alpha\gamma_{ab}/(\Omega_2 - \Omega_1), \quad (6)$$

where α is a linear function of the excitation η and also a function of the mode spacing $\Omega_2 - \Omega_1$. The dashed curves in Fig. 9 are calculated from Eq. (6). The threshold beat frequency is the same as for the independent mode calculation. The effect of the interaction is to cause the frequencies of oscillation to move farther apart than is predicted by the simpler calculation as the excitation increases. The value of γ_{ab}/Ku which gives an initial slope equal to that measured evidently lies between 0.04 and 0.08. The value of γ_{ab}/Ku required to fit the measurements would have been larger had a smaller Doppler width been assumed.

While hole-repulsion effects are minimum at threshold for the symmetric case, this is not true for situations where oscillation is already present at one frequency as a second mode crosses threshold. In Fig. 5 the threshold beat frequency for cavity mode placements other than symmetric exceeds the symmetric threshold beat frequency by an amount larger than predicted on the basis of no interaction of modes. This discrepancy appears to increase as the modes are tuned away from the symmetric condition at least until one mode is sufficiently close to line center that the decrease of frequency pushing of that mode due to its own hole makes it difficult to infer any additional pushing due to the second mode.

An experiment to measure γ_{ab}/Ku is suggested by Eq. (6). It consists of varying the maser mirror spacing and consequently $\Omega_2 - \Omega_1$ until the beat frequency between two adjacent modes symmetrically placed about line center is found to be independent of excitation. Then, if $\Omega_2 - \Omega_1 = \Delta$,

$$\frac{\gamma_{ab}}{Ku} = -\frac{\Delta/2 Z_r(\Delta/2, \gamma_{ab}, Ku)}{Ku Z_i(\Delta/2, \gamma_{ab}, Ku)}, \quad (7)$$

where Z_r and Z_i are the real and imaginary parts of a function related to the probability integral for complex argument and which are defined by Lamb.¹ The solution

⁸H. Haken and H. Saueremann, Z. Physik **173**, 261 (1963); **176**, 47 (1963).

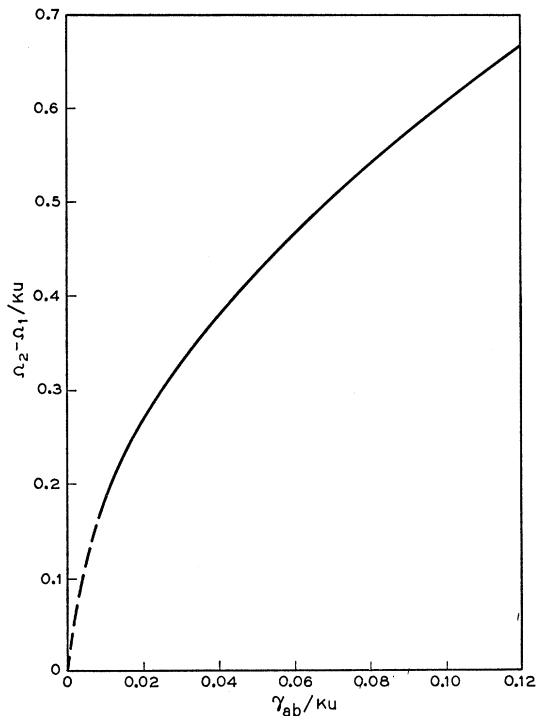


FIG. 10. Cavity-mode spacing for excitation-independent beat frequency when two resonances are symmetrically placed with respect to line center. Mode interaction effects have been included in the calculation.

of Eq. (7) is plotted in Fig. 10 where the mode spacing $\Omega_2 - \Omega_1$ appropriate to a given γ_{ab} is indicated.⁹

An effect appears in Fig. 5 curve (a) which is not predicted by either Eq. (1) or (4). These two equations show the beat frequency to be a linear function of excitation η . At higher excitation levels, however, curve (a) Fig. 5 changes from negative to positive slope and a description linear in η is no longer adequate. The effect cannot have been directly due to a decrease of gain with excessive rf excitation as the beat note did not disappear as it crossed its threshold value for the second time. The direction of the change in slope is consistent with an increase of γ_{ab} or effective linewidth of the transition. If collisions with atoms in other excited states were responsible for increasing the phenomenologically introduced decay rates γ_a or γ_b (γ_{ab} is equal to one-half the sum of γ_a and γ_b) such a dependence of γ_{ab} on excitation might be expected.

The author is indebted to Professor W. E. Lamb, Jr., for permission to read his manuscript prior to its publication and for discussion of its contents. The

⁹ It has been pointed out by R. L. Fork that this proposed measurement is complicated by the effects of mode competition when two modes are oscillating with parallel polarizations as in the case of a Brewster window configuration. Since this is, in fact, the situation assumed in the derivation of Lamb's theory, Eq. (7) cannot accurately describe the present experiment where the polarizations were orthogonal and no instabilities due to mode competition were apparent.

polarization studies were carried out in collaboration with W. L. Faust. Profitable discussions with A. Javan during the course of the experiments are gratefully acknowledged. Thanks are due to D. E. Thomas for the details of the interpretation of the frequency pushing and pulling in terms of phase shifts determined from gain and loss curves.

APPENDIX

The frequency pulling and frequency pushing terms in Eq. (1) are determined by Lamb¹ as

$$\sigma = \frac{\nu}{2Q} \frac{Z_r(\Omega - \omega)}{Z_i(0)}, \quad (\text{A1})$$

and

$$\rho E^2 = \frac{\nu}{2Q} \left\{ \frac{Z_i(\Omega - \omega)}{Z_i(0)} - 1 \right\} \frac{\gamma_{ab}(\Omega - \omega)}{2\gamma_{ab}^2 + (\Omega - \omega)^2}, \quad (\text{A2})$$

where Z_r and Z_i are the real and imaginary parts of

$$Z(\nu - \omega) = 2i \int_{-\infty}^{\xi} dt \exp -(\ell^2 + \zeta^2), \quad (\text{A3})$$

$$\zeta = \frac{\nu - \omega}{Ku} + i \frac{\gamma_{ab}}{Ku},$$

and ν/Q is the bandwidth of the optical resonator.

It is instructive to consider the significance of each of these terms by examining a model to which can be applied a "hole-burning" type of analysis as used by Bennett.² The model consists of a feedback loop made up of four elements: a medium with a frequency-dependent gain, a transmission type resonant cavity with a specified bandwidth and maximum transmission on resonance, two frequency-dependent loss elements to represent the presence of two holes in the gain curve. The last two elements have frequencies of maximum loss as follows: one at the oscillation frequency and the other on the opposite side of line center and equally far away from it. Off their respective resonances these elements approach unity gain and have bandwidths defined by twice the natural linewidth of the transition.¹⁰ The frequency of oscillation is determined by the requirement of zero net phase shift around the feedback loop.

The gain and phase shift of a Doppler broadened line with a line center gain of 1 neper is plotted in Fig. 11 where effects of natural linewidth are omitted. The gain of the medium in nepers is simply

$$e^{-[\Omega - \omega / Ku]^2} = \frac{Z_i(\Omega - \omega)}{Z_i(0)} \Big|_{\gamma_{ab}=0} \quad (\text{A4})$$

¹⁰ The hole width in the gain profile is twice the hole width in the velocity profile. See W. R. Bennett, Jr., in *Proceedings of the Third International Conference on Quantum Electronics*, edited by P. Grivet and N. Bloembergen (Columbia University Press, New York, 1964), p. 453.

$$2\Delta\omega_{nat} = 2(\gamma_a + \gamma_b) = 4\gamma_{ab}$$

and it can be shown¹¹ that the phase shift for such a gain profile is

$$\theta(\Omega - \omega) \Big|_{1 \text{ neper}} = \frac{Z_r(\Omega - \omega)}{Z_i(0)} \Big|_{\gamma_{ab}=0}. \quad (\text{A5})$$

For line center gains other than 1 neper the phase is equal to the line center gain in nepers times the phase for 1 neper.

If G_m is the numerical gain of the medium and G_c is the resonant transmission gain ($G_c < 1$) of the optical cavity and G_{mn} and G_{cn} are their values in nepers, it can be shown that

$$G_{mn} = -G_{cn}\eta \frac{Z_i(\Omega - \omega)}{Z_i(0)} \Big|_{\gamma_{ab}=0}, \quad (\text{A6})$$

where η is defined to be \bar{N}/\bar{N}_T as before. The phase associated with this gain is therefore

$$\theta_m = -G_{cn}\eta \frac{Z_r(\Omega - \omega)}{Z_i(0)} \Big|_{\gamma_{ab}=0}. \quad (\text{A7})$$

From an analysis based on lumped circuit elements,¹² it follows that a transmission resonant cavity with a

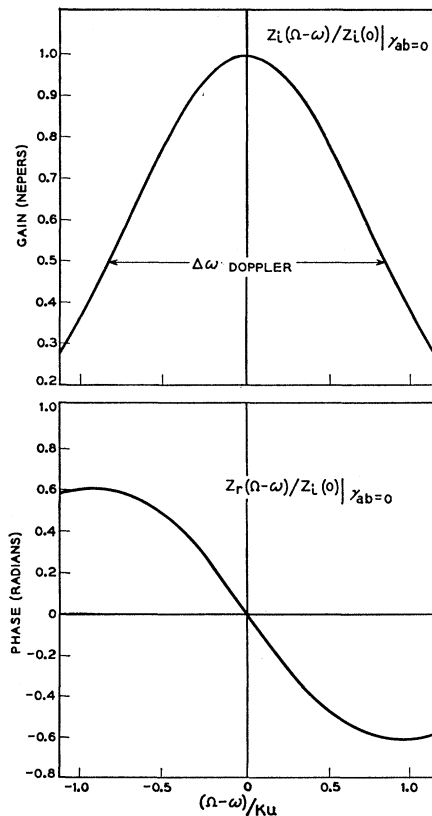


FIG. 11. Doppler broadened gain profile and its associated phase shift.

¹¹ D. E. Thomas, Bell System Tech. J. 42, 637 (1963).

¹² C. G. Montgomery, R. H. Dicke, and E. M. Purcell, *Principles of Microwave Circuits*, MIT Radiation Laboratory Series, Vol. 8 (McGraw-Hill Book Company, Inc., New York, 1948), p. 238.

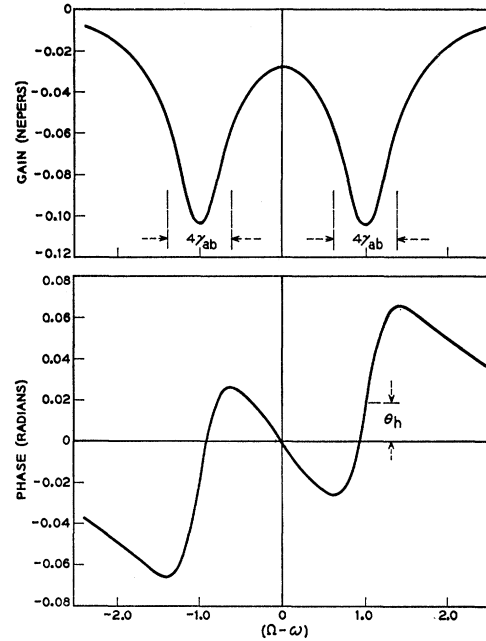


FIG. 12. The frequency-dependent gain associated with two holes and the related phase shift. The gain at the center of each hole has been arbitrarily set equal to -0.1 neper. θ_h is the residual phase at the frequency of oscillation and is due entirely to the complementary hole.

resonant power gain $G_c < 1$ and specified Q has a phase shift defined by

$$\theta_c = \arctan[-(2Q/\nu_0)(1 - \sqrt{G_c})(\nu - \nu_0)]. \quad (\text{A8})$$

At frequencies much less than resonance $\theta_c = \frac{1}{2}\pi$ and at frequencies much greater than resonance $\theta_c = -\frac{1}{2}\pi$. The phase is zero at $\nu = \nu_0$ and because of the high Q has a very steep slope at line center compared to the other resonant elements in the loop. Frequency pulling effects are a small fraction of the cavity bandwidth and equating the arctangent to its argument near line center we find

$$d\theta/d\nu = -(2Q/\nu_0)(1 - \sqrt{G_c}). \quad (\text{A9})$$

Since $G_c \approx 1$, $(1 - \sqrt{G_c}) \approx -\frac{1}{2}G_{cn}$ and

$$d\nu/d\theta = (\nu_0/Q)(1/G_{cn}). \quad (\text{A10})$$

To offset a phase θ_m due to the medium the oscillation frequency ν must move to cause the cavity to introduce a phase $-\theta_m$. That is,

$$\Delta\nu_m = \frac{\nu_0}{Q} \eta \frac{Z_r(\Omega - \omega)}{Z_i(0)} \Big|_{\gamma_{ab}=0}, \quad (\text{A11})$$

where $\Omega \approx \nu \approx \nu_0$. This agrees within a factor of 2 with Eq. (A1) for the case of zero natural linewidth. The functions Z_r and Z_i are modified from the above when $\gamma_{ab} \neq 0$ as a result of the introduction of a complex frequency into their arguments. Bennett's results² become identical to Eq. (A11) when a factor of 2 error in his Eq. (13) is corrected.

The gain and associated phase profile for two holes is shown in Fig. 12. Since the holes appear in the velocity profile and not strictly in the gain versus frequency curve we can consider that there is one "oscillating" hole near the cavity resonant frequency and a complementary "nonoscillating" hole placed the same distance on the other side of line center. The presence of the hole at the oscillation frequency introduces no additional phase shift into the feedback loop and the phase at $\nu \approx \Omega$ marked θ_h in Fig. 12 is due entirely to the complementary hole.

Defining the hole power gain as $G_h < 1$ and noting the loop requirement that

$$G_{mn} + G_{cn} + G_{hn} = 0, \quad (\text{A12})$$

we find

$$G_{hn} = G_{cn} \left\{ \eta \frac{Z_i(\Omega - \omega)}{Z_i(0)} \Big|_{\gamma_{ab}=0} - 1 \right\}. \quad (\text{A13})$$

From a lumped circuit element analysis similar to that used above, it follows that a complementary Lorentzian hole of width $4\gamma_{ab}$ introduces a phase at Ω defined by

$$\theta_h = \arctan \frac{[1 - \sqrt{G_h}](\Omega - \omega)/\gamma_{ab}}{1 + \sqrt{G_h}(\Omega - \omega)^2/\gamma_{ab}^2}. \quad (\text{A14})$$

For small cavity losses $-G_{cn} \ll 1$ and so therefore is $-G_{hn}$.

$$\begin{aligned} 1 - \sqrt{G_h} &\approx -\frac{1}{2}G_{hn} \\ \sqrt{G_h} &\approx 1. \end{aligned}$$

The arctangent is, therefore, approximately equal to its argument and

$$\begin{aligned} \theta_h &\approx \frac{-G_{hn}}{2} \frac{\gamma_{ab}(\Omega - \omega)}{\gamma_{ab}^2 + (\Omega - \omega)^2} \\ &= \frac{-G_{cn}}{2} \left\{ \eta \frac{Z_i(\Omega - \omega)}{Z_i(0)} \Big|_{\gamma_{ab}=0} - 1 \right\} \frac{\gamma_{ab}(\Omega - \omega)}{\gamma_{ab}^2 + (\Omega - \omega)^2}. \quad (\text{A15}) \end{aligned}$$

To offset θ_h , the oscillation frequency must move an amount such that the cavity provides an amount of phase equal to $-\theta_h$.

$$\Delta\nu_h = \frac{\nu_0}{2Q} \left\{ \eta \frac{Z_i(\Omega - \omega)}{Z_i(0)} \Big|_{\gamma_{ab}=0} - 1 \right\} \frac{\gamma_{ab}(\Omega - \omega)}{\gamma_{ab}^2 + (\Omega - \omega)^2}. \quad (\text{A16})$$

This term is similar to ρE^2 calculated by Lamb differing significantly only for a cavity resonance near line center where the two holes overlap. It appears to represent a hole repulsion effect between the "oscillating" and "nonoscillating" hole.

Superconductivity in a Strong Spin-Exchange Field*

PETER FULDE AND RICHARD A. FERRELL

University of Maryland, College Park, Maryland

(Received 23 December 1963; revised manuscript received 17 April 1964)

A strong exchange field, such as produced by ferromagnetically aligned impurities in a metal, will tend to polarize the conduction electron spins. If the metal is a superconductor, this will happen only if the spin-exchange field is sufficiently strong compared to the energy gap. When the field is strong enough to break many electron pairs, the self-consistent gap equation is modified and a new type of depaired superconducting ground state occurs. In the idealization of a spatially uniform exchange field with no scattering, it is found that the depaired state has a spatially dependent complex Gorkov field, corresponding to a nonzero pairing momentum in the BCS model. The presence of the "normal" electrons from the broken pairs reduces the total current to zero, gives the depaired state some spin polarization, and results in almost normal Sommerfeld specific heat and single-electron tunneling characteristics. The nonzero value of the pairing momentum also gives rise to an unusual anisotropic electrodynamic behavior of the superconductor, as well as to a degenerate ground state and low-lying collective excitations, in accordance with Goldstone's theorem. The effects of scattering in an actual superconducting ferromagnetic alloy have not been studied and may interfere with experimental investigation of the theoretical results found in this paper for the idealized model.

I. INTRODUCTION

THERE is experimental evidence of ferromagnetic alignment of paramagnetic impurities when they are in the form of a dilute solution, dissolved in certain

nonmagnetic metals. A typical example is the recently reported¹ ferromagnetism of 0.8% of iron dissolved in gold, which has been found to exhibit a Curie temperature of 9°K. In some cases, when the host metal becomes a superconductor at sufficiently low temperature, there

* Research supported in part by the U. S. Air Force Office of Scientific Research and by ARPA. This work forms a portion of a thesis submitted by one of the authors (Peter Fulde) to the faculty of the University of Maryland in partial fulfillment of the requirements for the Ph.D. degree.

¹ R. J. Borg, R. Booth, and C. E. Violet, Phys. Rev. Letters **11**, 465 (1963). *Note added in proof.* For an alternative interpretation of this experiment, not involving ferromagnetic ordering, see J. Crangle and W. R. Scott, Phys. Rev. Letters **12**, 126 (1964).

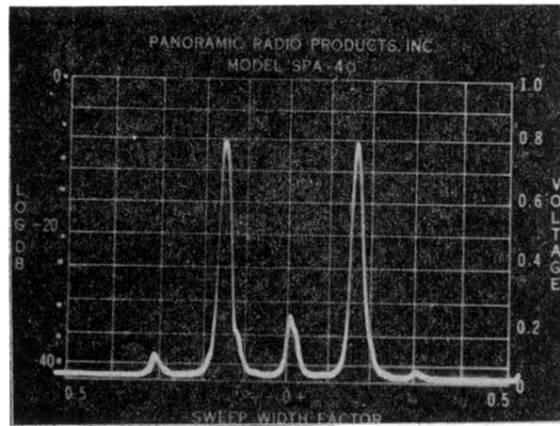


FIG. 2. Panoramic receiver display of five beat components at 306 Mc/sec. Total scan is approximately 20 kc/sec.